AC Losses in the First ITER CS Module Tests: Experimental Results and Comparison to Analytical Models

AC Losses in the First ITER CS Module Tests: Experimental Results and Comparison to Analytical Models

M. Breschi, *Senior Member, IEEE,* L. Cavallucci, P. L. Ribani, *Member, IEEE,* R. Bonifetto, *Member, IEEE*, A. Zappatore, *Associate Member, IEEE*, R. Zanino, *Senior Member, IEEE*, F. Gauthier, P. Bauer, and N. Martovetsky

***Abstract*—The ITER Central Solenoid (CS) will be manufactured by assembling a stack of six modules, which are under fabrication by the US ITER organization and its subcontractors. The tests of the first CS Module have been performed at the premises of the General Atomics (GA) facility in Poway (US), in order to check compliance to the ITER requirements. Among other tests, the magnet was submitted to exponential dumps of the transport current from different initial values (10, 15, 20, 22.5, 25, 35, 40 kA) down to 0 kA. These tests are aimed at conducting DC breaker commissioning of the test facility and were used to measure the AC losses in the coil during electrodynamic transients. This paper presents the results of these measurements, along with a comparison with analytical computations of the losses in the magnet.**

***Index Terms*—AC Losses, Cable in Conduit Conductors, Central Solenoid, ITER project.**

I. Introduction

The losses in superconducting coils during electrodynamic transients are of paramount importance for a correct dimensioning of their cryogenic circuit. Several experimental, numerical and analytical studies have been presented on this topic in the recent years [1] - [8]. This paper focuses on the analysis of electrodynamic losses in the first module of the Central Solenoid of the ITER magnet system [9], which consists of 40 pancakes wound with a Nb_3Sn Cable in Conduit Conductor (CICC) [10]. The tests of the first module (CSM#1) were performed at the premises of General Atomics (GA), in Poway, close to San Diego (US) [11]. The AC loss measurements were performed by de-energizing the magnet through exponential dumps of the transport current, from different initial values, namely 10, 15, 20, 22.5 25, 35, 40 kA. The paper presents the results of these tests, obtained by computing the heat deposited in the supercritical helium of the cryogenic system with two methodologies, namely a calorimetric and an isochoric approach. It should be noted that the AC losses in the CS JASTEC conductor, which is the same used for the CSM#1, were previously measured in a straight configuration in the SULTAN facility (SPC, Switzerland) [12], and in a single-layer solenoid configuration (CS Insert, or CSI) in the CS Model Coil facility (QST, Naka, Japan) [13], [14]. This paper presents a comparison between the experimental data and the results of analytical models, based on parameters calibrated on these previous tests.

II. Experimental Set-up

The CSM#1 consists of 20 double-pancakes cooled by supercritical helium, as sketched in Fig. 1. The module is supported by a 10 tons stainless-steel frame, positioned at the bottom of the magnet.

The CSM#1 cryogenic circuit is equipped with several control valves: CV4 is located at the outlet of pancake #1; CV3 at the outlet of the set of pancakes from #2 to #38, CV5 at the outlet of pancake #40 and CV6 at the outlet of the coil frame. The valve CV2 is a coil by-pass valve allowing the recirculation of helium from the outlet of the cold circulator directly to the outlet of the module.

The thermal-hydraulic instrumentation of CSM#1 is reported in Fig. 1, and includes temperature, pressure and mass flow rate sensors, placed in the cryogenic loop at the inlet of all the pancakes and at the common outlet of pancakes from #2 to #39. The helium at the outlet of pancakes #1 and #40 is used for the cooling of the terminal joints; pressure and mass flow rate are monitored downstream the In-Cryostat-Feeder and joint, whose contributions are subtracted. The measurements of AC losses are mainly aimed at assessing the electrodynamic losses in the set of pancakes from #2 to #39.

The AC loss tests are performed at the beginning of the test campaign (no electromagnetic cycles performed) by ramping up the transport current with a slow linear ramp up to the peak value, ranging from 5 kA to 40 kA. After an operation current

The work at Università di Bologna was supported by the ITER Organization under contract # IO/17/CT/4300001613. *(Corresponding author: Marco Breschi).*

The work at Politecnico di Torino was supported by UT-Battelle, LLC, under subcontract #4000148178. The work of A. Zappatore was partially supported by the Euratom research and training program 2014-2018 and 2019-2020 under grant agreement No 633053.

M. Breschi, L. Cavallucci and P.L Ribani are with the Department of Electrical, Electronic and Information Engineering, Università di Bologna, Italy (e-mail: marco.breschi@unibo.it).

P. Bauer and F. Gauthier are with the ITER Organization, Cadarache, France.

R. Bonifetto, A. Zappatore, R. Zanino are with the NEMO Group, Dipartimento Energia, Politecnico di Torino, Italy.

N. Martovetsky is with Lawrence Livermore National Laboratory, on assignment to Oak Ridge National Laboratory, USA.

flat top of a few hundred seconds, the magnet is discharged on a resistor bank.

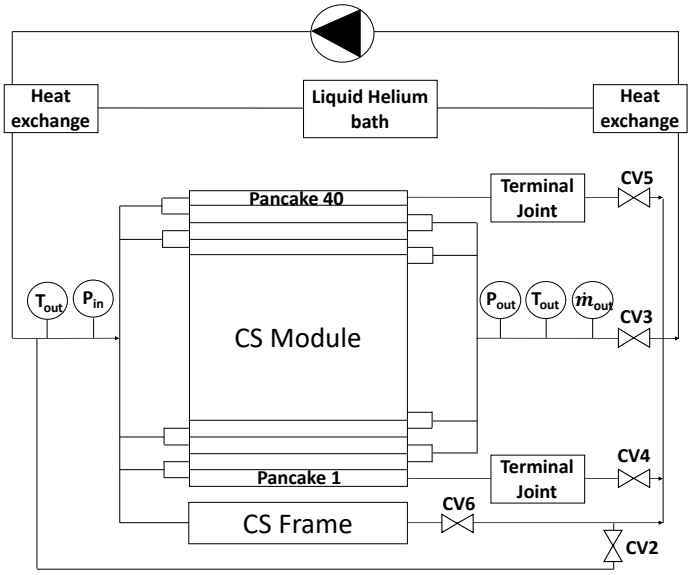

Fig. 1. Sketch of the CSM1 instrumentation.

It should be noted that the AC loss tests themselves might affect the contact resistances between strands, so that the conductor properties may evolve during the test campaign. Given the overall coil inductance of 795 mH and a resistor bank resistance of 103 mΩ, the nominal current dump time constant is ~7.8 s.

Two different configurations of the cryogenic loop were adopted. For dumps from operation currents below (or equal to) 25 kA, the control valves are not operated, thus leaving the helium circulator connected to the coil during the current discharge. During the dumps from higher current values, such as 35 and 40 kA, the helium circulator is protected by opening the control valve CV2 that connects the helium inlet line with the helium outlet line, and closing the valves CV3, CV4, CV5 and CV6 on the outlet line. This operation allows short circuiting the circulator and bypassing the coil.

A typical set of signals recorded during an exponential dump is reported in Fig. 2, which refers to the initial operation current of 20 kA. The mass flow rate is shown in Fig. 2a. Due to the large heat deposition, the total mass flow rate measured at the outlet of the coil gets rather low for a few seconds and then it recovers its nominal value. This initial drop is due to the pressure rise in the cryogenic circuit, induced by the heat deposition in the coil, which propagates throughout the entire circuit, thus also increasing the outlet pressure (see Fig. 2(b)). The evolution of the temperature at the coil outlet during the dump is shown in Fig. 2(c). The frequent but irregular mass flow rate perturbations (see e.g. Fig. 2(a) around 900 and 1500 s) are due to oscillations in the entire cryogenic loop not related to the tests analyzed here.

III. Assessment of AC Losses from Experiments

The computation of the energy deposited in the supercritical helium during the dumps was performed according to two different approaches, namely a calorimetric and an isochoric method.

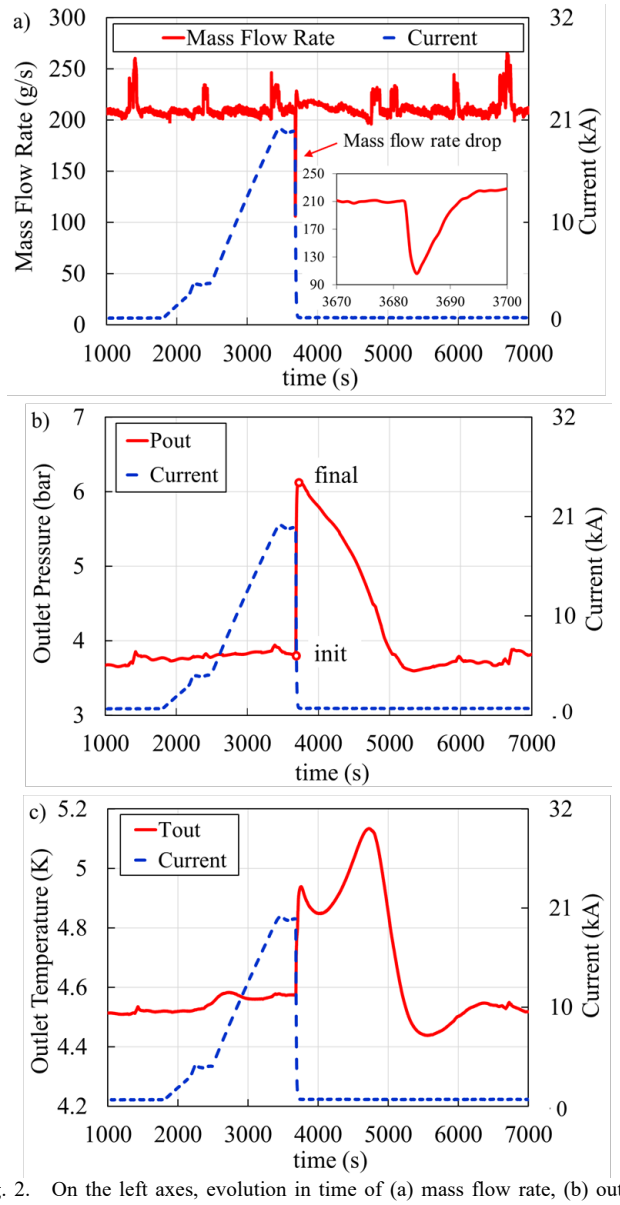

Fig. 2. On the left axes, evolution in time of (a) mass flow rate, (b) outlet pressure and (c) outlet temperature during the dump at 20 kA. On the right axes the current profile is shown.

A. Calorimetric Method

The calorimetric method is based on the integration over time of the power deposited into the cryogenic fluid. The formula used for computation is the following:

$$E = \int_{t_0}^{t} \{\dot{m}_{out}(t) \cdot [h(p_{out}(t), T_{out}(t)) - h(p_{in}(t), T_{in}(t))] - P_0\}\, dt \quad (1)$$

where $\dot{m}_{out}$, p_{out}, and T_{out} are the mass flow rate, pressure and temperature at the outlet, respectively, p_{in} and T_{in} the corresponding values of pressure and temperature at the inlet, h the helium specific enthalpy as a function of pressure and temperature. The time of integration spans from the instant just before the beginning of the dump to the recovery of steady conditions, i.e. after the He transit-time in the coil (~1500 s). The power P_0 is an offset, calculated as the difference between the enthalpy at

the outlet and at the inlet at a selected time t_0, taken just before the triggering of the current dump, as follows:

$$P_0 = \dot{m}_{out}(t_0) \cdot [h\big(p_{out}(t_0), T_{out}(t_0)\big) - h\big(p_{in}(t_0), T_{in}(t_0)\big)] \quad (2)$$

For the dumps from transport current values above 25 kA, the aforementioned valve operation determines a drop of the inlet pressure and remarkable variations of the mass flow rate, which make this assessment not reliable.

B. Isochoric Method

Given the very fast pressure rise of the supercritical helium embedded in the module during the current dump, an isochoric method was developed. In the isochoric method, the heat deposition is computed as follows:

$$Q = m_{He}\big[U\big(p_{final}, T_x\big) - U(p_{init}, T_{init})\big] \quad (3)$$

where m_{He} is the helium mass in the coil (in this case equal to 263.7 kg); U is the helium internal energy as a function of pressure and temperature; p_{init} and T_{init} are respectively the temperature and pressure at time t_0 before the dump; p_{final} is the pressure immediately after the current dump and T_x is the average temperature of the helium inside the module at the end of the dump. This value is computed according to the isochoric assumption of constant specific volume and hence of constant density during current dumps. The temperature T_x fulfils the following relation:

$$\rho\big(p_{final}, T_x\big) = \rho(p_{init}, T_{init}) \quad (4)$$

where ρ is the helium density.

The large outlet pressure variation of the helium in the module before and after the dump from 20 kA is shown in Fig. 2(b).

The isochoric method is based on the assumptions that a) the energy is totally deposited in the He, b) the He mass is the same at the two instants considered, c) the pressure and temperature are uniform within the coil.

a) The heat capacity of the solids is negligible (at low temperature) with respect to that of the He, i.e ~ 10^3 J/K vs. 10^6 J/K. Also, the heat transfer between He and solids acts over a time constant shorter than the time interval considered, i.e. ~ 30 s; therefore the solid and He temperatures are very close.

b) The total He mass in the coil is ~260 kg. The measured He mass exiting the coil during the dump (if the coil is not isolated, i.e. when the initial current is below or equal to 25 kA) is ~1.5 kg. A similar contribution is entering the coil at its inlet, since backflow only occurs for a few seconds. When the coil is isolated, the helium is trapped inside the coil several seconds before dump starts, and circulation is restored about 10 s seconds after the end of dump: in this case the helium is not escaping the coil during the dump.

c) The pressure equilibrates at the speed of sound; considering ~150 m/s in the hydraulic channel, it takes a few seconds to get equilibrium in the pressure, so that transient effects on the pressure along the hydraulic channel are thus negligible. The pressure drop along the coil (for the dumps without coil isolation), is ~ 0.3 bar.

The application of the isochoric method to the computed results might lead to an underestimation of the deposited energy of ~ 15 %. Note that this error is mainly due to assumption c), while assumptions a) and b) give negligible error.

IV. Analytical Models

A. Coupling Losses

The analytical calculation of the coupling losses was performed according to the Single Time Constant Model (STCM) [15]. The study performed through the STCM extrapolates to the CSM#1 the results of the analysis of the CS Insert [16], [17] and that of the CS conductor in the straight configuration [12] in the SULTAN facility [18]. In this model, the power per unit volume (W/m^3) is computed as:

$$P_{coup}(t) = \frac{n\tau}{\mu_0} \cdot \left(\dot{B}_i(t)\right)^2 \quad (5)$$

where $\dot{B}_i$ is the time derivative of the internal magnetic flux density and τ is the cable time constant. Further details on this computation methodology can be found in [13]-[15]. The conductor $n\tau$ as derived from the analysis of the CS Insert test campaign depends on the value of the initial current [13]. For the calculations reported here, the value of $n\tau$ is set to 570 ms, corresponding to the dump in the CS Insert from 37 kA [13]. The value of $n\tau$ was also derived from the aforementioned tests in SULTAN, performed at background fields of 2 T and 9 T. These tests allowed to derive an expression of $n\tau$ for the conductor in virgin conditions as a function of magnetic flux density, which also extrapolates correctly to the value of $n\tau$ found on the same conductor at the University of Twente at 0 T ($n\tau$ = 573 ms). An additional term, also derived from the tests at the University of Twente, accounts for the impact on losses of the Lorentz force ($I \cdot B$), thus resulting in the following expression:

$$n\tau\,[s] = 0.573 - 0.0179 \cdot \mathrm{B\,[T]} + 1.45\ 10^{-4}\ (I \cdot B)[kA\ T] \quad (6)$$

The results of the calculations performed by extrapolating with a constant $n\tau$ = 570 ms from the CS Insert test results and with the variable $n\tau$ described in (6) are reported in the next sections.

B. Hysteresis Losses

The computation of hysteresis losses starts from the calculation of the penetration field B_p [19] at each location of the CSM#1:

$$B_p = \frac{\mu_0\, \lambda\, J_c(B, T, \varepsilon)\, d_{eff}}{\pi} \quad (7)$$

where λ is the ratio betwen the non-copper area and the filament area (λ = 2.36), d_{eff} is the effective filament diameter (d_{eff} = 14 μm) and $J_c(B, T, \varepsilon)$ is the critical current density as a function of magnetic flux density B, temperature T and effective strain ε.

The hysteresis losses in the k-th turn, $P_{hys,k}$, are computed with two different formulae depending on the value of the cumulative field variation in that turn, ΔB_k. In case $\Delta B_k < 2B_p$, the following formula is adopted [19]:

$$P_{hys,k} = \big(N_{str}\, A_{fil} \cdot L_k\big) \frac{\Delta B_k^2}{2\mu_0 B_p} \frac{dB_k}{dt} \left(1 - \frac{\Delta B_k}{3\, B_p}\right) \quad (8)$$

where N_{str} is the number of superconducting strands (N_{str} = 576) A_{fil} is the area occupied by the superconducting filaments in each 0.83-mm-diameter strand, and L_k the length of the twisted conductor along the k-th turn. Instead, if $\Delta B_k > 2B_p$, the following relation is used [15], [19]:

$$P_{hys,k} = \left(N_{str}\, A_{fil} \cdot L_k\right) \frac{2}{3\pi}\, \lambda\, J_c(B_k, T, \varepsilon)\, d_{eff}\, \frac{dB_k}{dt} \quad (9).$$

C. Model results

The analytical calculations allow computing the loss distribution in the various pancakes of the magnet. As an example, Fig. 3 shows the hysteresis and coupling loss distribution in the CSM#1 for the dump from 40 kA. The hysteresis losses are significantly lower than the coupling losses in all pancakes. A rather good agreement is found between the data extrapolated from the CSI test results and from the SULTAN tests (with the variable time constant reported in (6)).

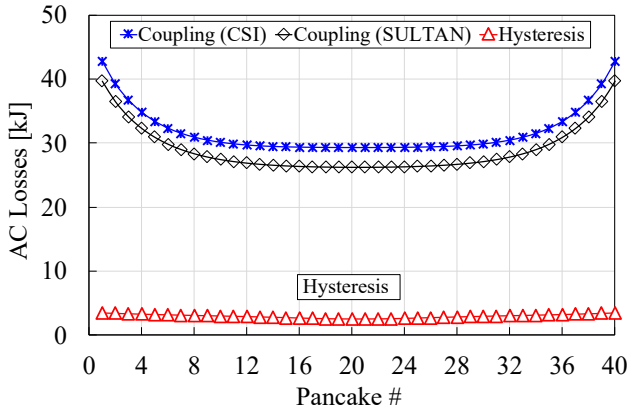

Fig. 3. Coupling losses distribution in the CSM#1 during dump from 40 kA.

V. Experimental Results and Discussion

A. Losses in the frame

During the operation current dumps, the steel frame is also subjected to a time varying magnetic field, which generates eddy currents and related losses. A calorimetric analysis of a series of six consecutive dumps shows that while 1.7 MJ are deposited in the frame, only 50 kJ are deposited in pancake #1. The total amount of heat deposited in the set of pancakes from #2 to #39 is 1.75 MJ, which corresponds to about 44 kJ per pancake. This result shows that even in pancake #1, the closest to the frame, the deposited heat does not significantly deviate from the values found for the other pancakes. It can therefore be concluded that eddy current losses in the steel frame have a negligible impact on the calorimetry of the set of pancakes from #2 to #39.

B. Losses in the coil

The experimental results of losses obtained in the dumps from 10 to 40 kA are reported in Fig. 4. The losses computed with the isochoric method are on average 25 % lower than those found with the calorimetric procedure, which is acceptable considering the sensors accuracy and the assumptions involved in both methodologies.

The losses computed with the analytical models are also plotted in Fig. 4. The results based on the extrapolation from the CSI tests and from the tests in SULTAN (see (6)) are in good agreement with each other. Maximum differences of 13 % and 34 % (at 15 kA) are found between the computations from the CS Insert data and the experimental results obtained with the isochoric and the calorimetric method respectively.

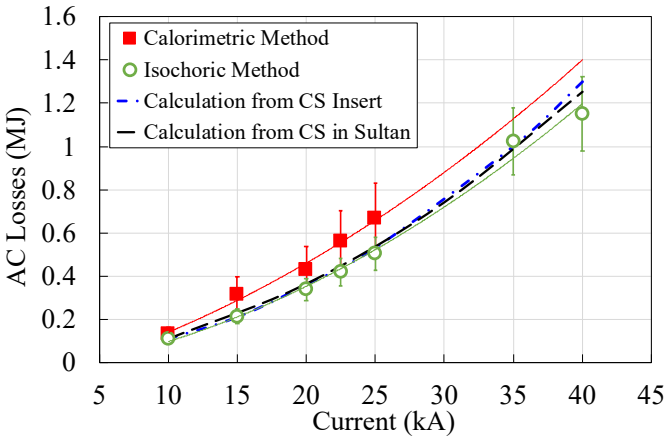

Fig. 4. AC Losses in the CSM#1. The experimental results obtained with the calorimetric and the isochoric procedures are compared with the analytical calculations from the tests of the CSI and the SULTAN sample CSJA6.

VI. Conclusion

The tests of AC losses in the first module of the ITER Central Solenoid were successfully performed through exponential dumps of the transport current, starting from different values in the range from 10 to 40 kA. The losses in the coil at the beginning of the test campaign were estimated with both a calorimetric and an isochoric method, finding a 25 % difference between the results of the two methods. Although large eddy current losses in the frame were also detected, these do not affect the assessment of the losses in the superconducting coil.

Considering the significant scale-up from the short sample tested in SULTAN (~ 4 m long conductor), and from the single – layer solenoid tested in the CS Insert (~ 45 m), to the CS Module magnet (~ 6 km), and the assumptions involved in the analytical models and in the derivation of the experimental results, the agreement between calculations and measurements is deemed satisfactory.

Acknowledgment

The authors wish to thank the dedicated team of General Atomics for the experimental tests and technical assistance. Useful discussions on the analytical modeling with B. Turck and J. L. Duchateau (formerly at CEA Cadarache), and A. Torre (CEA Cadarache) are also gratefully acknowledged.

Disclaimer: The views and opinions expressed herein do not necessarily reflect those of the ITER Organization or of the European Commission.

REFERENCES

[1] P. L. Bruzzone, "Superconductivity: hysteresis and coupling losses," in *Engineering Superconductivity*, P. J. Lee, Ed. New York, NY, USA: Wiley Interscience, pp. 138–152, 2001.

[2] A. Nijhuis et al., "Optimization of interstrand coupling loss and transverse load degradation in ITER Nb3Sn CICCs," *Supercond. Sci. Technol.*, vol. 23, 2013, Art. no. 4201206.

[3] E. P. A. van Lanen, J. van Nugteren, and A. Nijhuis, "Full-scale calculation of the coupling losses in ITER size cable-in-conduit conductors," *Supercond. Sci. Technol.*, vol. 25, 2012, Art. no. 025012.

[4] A. Louzguiti, "Magnetic screening currents and coupling losses induced in superconducting magnets for thermonuclear fusion", Ph. D. Dissertation, Université d'Aix – Marseille, 2017.

[5] M. Chiletti, J. L. Duchateau, F. Topin, B. Turck, and L. Zani, "Analytical Modeling of CICCs Coupling Losses: Broad Investigation of Two-Stage Model," *IEEE Trans. Appl. Supercond.*, vol. 29, no. 5, 2019, Art. no. 4703005.

[6] A. Louzguiti, L. Zani, D. Ciazynski, B. Turck, J. L. Duchateau, A. Torre, and F. Topin, "AC Coupling Losses in CICCs: Analytical Modeling at Different Stages," *IEEE Trans. Appl. Supercond.*, vol. 27, no. 4, 2017, Art. no. 0600505.

[7] B. Turck, L. Zani, "A macroscopic model for coupling current losses in cables made of multistage of superconducting strands and its experimental validation", *Cryogenics,* vol. 50, pp. 443-449, 2010.

[8] P. L. Bruzzone, A. Nijhuis, and H. H. J. ten Kate, "Contact resistance and coupling loss in cable-in-conduit of Cr plated Nb_3Sn strands," *Proc. MT-15*, Beijing, Oct. 1997. Science Press, pp. 1295–1298, 1998.

[9] N. Mitchell et al., "The ITER magnet system," *IEEE Trans. Appl. Supercond.*, vol. 18, no. 2, pp. 435–440, 2008.

[10] P. Libeyre et *al.*, "An optimized central solenoid for ITER," *IEEE Trans. Appl. Supercond.*, vol. 20, no. 3, pp. 398–401, 2010.

[11] N. Martovetsky, et al. "First ITER CS Module Test Results", Fus. Eng. Des., vol. 164, 112169, 2021.

[12] M. Breschi *et al.*, "Analysis of AC Losses in a CS Conductor Sample for the ITER Project," *IEEE Trans. Appl. Supercond.*, vol. 28, n. 3, 2018, Art. No. 5900205.

[13] M. Breschi *et al.*, "Analysis of AC Losses in the ITER Central Solenoid Insert Coil", *IEEE Trans. Appl. Supercond.*, vol. 27, n. 4, 2017, Art. No. 7762085.

[14] R. Bonifetto *et al.*, "Modeling the ITER CS AC Losses Based on the CS Insert Analysis", *IEEE Trans. Appl. Supercond.*, vol. 29, n. 5, 2019, Art. No. 4200907.

[15] M. N. Wilson, Superconducting magnets, Oxford University Press, 1983.

[16] N. Martovetsky et al., "ITER Central Solenoid Insert Test Results," *IEEE Trans. Appl. Supercond.*, vol. 26, n. 4, 2016, Art. No. 4200605.

[17] N. Martovetsky et al., "Characterization of the ITER CS conductor and projection to the ITER CS performance," *Fusion Engineering and Design* vol. 124, pp. 1–5, 2017.

[18] P. L. Bruzzone et al., "Methods, accuracy and reliability of ITER conductor tests in SULTAN," *IEEE Trans. Appl. Supercond.*, vol. 19, no. 3, pp. 1508–1511, 2009.

[19] D. Bessette, "Assessment of the conductor AC Losses in the CS modules", ITER I/O internal report, IDM XQB5DS, 10 Dec 2018.